Draft version March 8, 2016
Preprint typeset using LaTeX style emulateapj v. 5/2/11

arXiv:1603.02050v1 [astro-ph.SR] 7 Mar 2016

UNEXPECTED SERIES OF REGULAR FREQUENCY SPACING OF δ SCUTI STARS IN THE NON-ASYMPTOTIC REGIME – I. THE METHODOLOGY

M. Paparó[1], J. M. Benkő[1], M. Hareter,[1] and J.A. Guzik[2]

Draft version March 8, 2016

ABSTRACT

A sequence search method was developed to search regular frequency spacing in δ Scuti stars by visual inspection and algorithmic search. We searched for sequences of quasi-equally spaced frequencies, containing at least four members per sequence, in 90 δ Scuti stars observed by CoRoT. We found an unexpectedly large number of independent series of regular frequency spacing in 77 δ Scuti stars (from 1 to 8 sequences) in the non-asymptotic regime. We introduce the sequence search method presenting the sequences and echelle diagram of CoRoT 102675756 and the structure of the algorithmic search. Four sequences (echelle ridges) were found in the 5-21 d^{-1} region, where the pairs of the sequences are shifted (between 0.5-0.59 d^{-1}) by twice the value of the estimated rotational splitting frequency (0.269 d^{-1}). The general conclusions for the whole sample are also presented in this paper. The statistics of the spacings derived by the sequence search method, by FT and that of the shifts are also compared. In many stars, more than one almost equally valid spacing appeared. The model frequencies of FG Vir and their rotationally split components were used to reveal a possible explanation that one spacing is the large separation, while the other is a sum of the large separation and the rotational frequency. In CoRoT 102675756, the two spacings (2.249 and 1.977 d^{-1}) agree better with the sum of a possible 1.710 d^{-1} large separation and two or one times, respectively, the value of the rotational frequency.

Subject headings: stars: oscillations — stars: variables: Delta Scuti — techniques: photometric — space vehicles

1. INTRODUCTION

Delta Scuti stars could be very important targets of asteroseismology once mode identification is successfully performed. They lie on and above the main sequence with intermediate mass and spectral types between A2 and F5. Both radial and non-radial p-type and g-type modes are excited covering a wide range of frequencies between 5-50 d^{-1}, or even wider that was revealed in *Kepler* data by Balona & Dziembowski (2011). The appearance of the convective core introduces poorly known physical processes in the stellar interiors, such as convective overshoot, mixing of chemical elements and redistribution of angular momentum (Zahn 1992). The investigation of the latter processes has nowadays become an observational science (Kurtz et al. 2014; Saio et al. 2015). Both in KIC 1145123 and KIC 9244992 slightly different surface-to-core rotation velocities were found using g-mode triplets and even p-mode triplets and multiplets. The successful investigation of the δ Sct/γ Dor hybrids relies on the very slow rotation of these stars. The equatorial rotation velocity is found to be about 1 kms^{-1} and the mean rotational splitting is 0.0138 d^{-1}.

However, most of the δ Scuti stars are intermediate or fast rotators with $\approx$ 100-200 kms^{-1} equatorial rotational velocity. Due to the complexity of the oscillation spectra, their pulsation behavior is not fully understood, especially the rotation-pulsation interaction. The problems and prospects were reviewed before the CoRoT and *Kepler* space missions by Goupil et al. (2005). Mostly the perturbative theory was used in the interpretations. Despite the problems, in the last 20 years several attempts have been made to interpret the observed spectra of δ Scuti stars (see references in Fox Machado et al. 2006).

Lignières et al. (2006) showed that the rotation-pulsation interaction cannot be described using the perturbation theory for rapidly rotating stars. At the same time Roxburgh (2006) presented self-consistent two-dimensional models of main-sequence stars. Reese et al. (2006) and Suárez et al. (2010) pointed out that the most severe problems appear in stars that show very high surface velocities, such as δ Scuti and Be stars, or in stars where the surface rotates slowly, but in which the pulsation periods are of the same order as the rotation period, such as for SPB and γ Doradus stars.

After solving a basic convergence problem (Jackson et al. 2004; McGregor et al. 2007), the modeling of rapidly rotating stars greatly improved. The models revealed four families of modes (low frequency modes, whispering gallery modes, chaotic modes and island modes). The frequency spectrum of rotating stars is interpreted as the superposition of subspectra of different mode families. The island modes with a new definition of quantum numbers are predicted to have regular patterns in rapidly rotating stars (Lignières et al. 2008, 2009, 2010; Reese et al. 2008, 2009). Nowadays echelle diagrams have been derived for model calculations by Deupree (2011) and Ouazzani et al. (2015).

A much higher signal to noise ratio of the space missions (CoRoT – Baglin et al. 2006; Auvergne et al. 2009 and *Kepler* – Borucki et al. 2010) has yielded the detection of a much larger set of modes in δ Scuti stars, in some cases hundreds of modes. There is, however,

paparo@konkoly.hu
[1] Konkoly Observatory, MTA CSFK, Konkoly Thege Miklós út 15-17., H-1121 Budapest, Hungary
[2] Los Alamos National Laboratory, Los Alamos NM 87545 USA

still a discrepancy between the number of actually detected and theoretically predicted modes. A direct comparison of the detected and model frequencies does not give a unique solution for mode identification. The traditional mode identification methods using the color amplitude ratio and the phase differences (Garrido 2000; Viskum et al. 1998) can only be applied to a few of the detected frequencies and limits the advantage of space missions by ground-based possibilities.

Although the frequencies of the low radial order modes are out of the asymptotic regime so that solar-type regular frequency spacings are not expected, some underlying regularities in the frequency spectra have been found even from ground-based international campaigns (Handler et al. 1997; Breger et al. 1999). In the era of great expectation of space missions, (Dziembowski et al. 1998) wondered whether mode identification will not be even more difficult to obtain for δ Scuti stars. Barban et al. (2001) published their effort to develop an alternative method which does not involve any knowledge of a model in its first steps and uses very precise data, i.e. frequencies, rather than amplitudes and phases. Model frequencies were used with realistic amplitude distribution based on visibility effects. Their echelle diagram is nicely regular in the high frequency region ($f > 35$ d^{-1}) but the echelle ridges are mixed in the low frequency region ($f < 35$ d^{-1}). Using a different $\Delta\nu$ value, some regularity appeared in the low frequency region, too, showing one straight and two highly inclined echelle ridges. After introducing the rotational splitting, the frequency spacing histogram no longer shows the peak at the large separation frequency, unless only the high amplitude and high frequencies are used.

Based on MOST data (Matthews 2007), CoRoT data (García Hernández et al. 2009, 2013; Mantegazza et al. 2012) and *Kepler* data (Breger et al. 2011; Kurtz et al. 2014) successful investigations were done for individual δ Scuti stars. Recently García Hernández et al. (2015) reported investigation of frequency spacing on a sample of 15 *Kepler* δ Scuti stars, obtaining a large separation for 11 stars. Their work flow shows that they use the Fourier Transform (FT) to find the large separation and, in ambiguous cases, they make a decision based on the histogram of the frequency differences. Knowing the frequency spacing, the echelle diagram is derived. In the echelle diagram for their sample case, KIC 1571717, two echelle ridges contain 6 and 4 frequencies, while on the other echelle ridges only three or even fewer frequencies are located.

We aimed to find a complementary method for searching for series of regular frequency spacing in a large sample of δ Scuti stars and for finding similarities or differences between the individual targets. We intended to use only the frequencies of high precision obtained by the space mission(s) similar to Barban et al. (2001), but finally we also used the amplitudes at the starting point.

2. SEARCH FOR SEQUENCES

The motivation for searching for sequences among the frequencies is twofold. Neither the histogram of frequency differences nor the FT give information on the connections between the frequencies. Only the most frequent spacing can be given, although the echelle diagram plotted later with the spacing shows which frequencies are located on the same ridge. Published examples show that the highest peak of the FT sometimes agrees with half of the large separation and not with the large separation itself that was obtained by modeling. On the other hand, avoiding any additional ground-based requirement for mode identification (nowadays we have too many targets but limited telescope time) we must know which frequencies are related to each other, for example, as in the sequence of eigenmodes with the same l value.

A personal motivation was our result on the δ Scuti star CoRoT 102749568 (Paparó et al. 2013). The frequency difference of the dominant modes and the period ratio, consistent with the radial fundamental and first overtone, yielded a relative identification of 12 frequencies having three different degrees, l. They did not show a comb-like structure, as in the asymptotic regime, but they were regularly interwoven. A paper by Chen & Li (2015) recently appeared on astro-ph that gave an interpretation with rotationally split modes, but there is no doubt about the regular spacing.

The large databases of space missions (CoRoT, *Kepler*) allow us great possibilities to search for any regularity in the frequency distribution that could help to derive the large separation or to resolve the interaction of rotation and pulsation in the non-asymptotic regime. We introduce in this paper the visual inspection and algorithmic approaches of the sequence search method.

2.1. *Visual inspection (VI)*

Visual inspection of the frequencies uses the ability of the human brain for searching for structure(s) in a seemingly unstructured sample. Both observational (Breger et al. 2009) and theoretical investigations (Suárez et al. 2014) have reported that the frequency differences between successive radial orders are not constant, but form a quasi-periodic structure at low radial order. A standard deviation of such a structure is roughly 2.5 μHz (0.216 d^{-1}) (García Hernández et al. 2009), which allowed us to look for non-strictly equidistant structures.

Visual inspection of the frequencies in the target stars proved to be a time-consuming but flexible way of searching for sequences with quasi-equidistant frequencies. The goal was to find criteria for an algorithmic search. In the asymptotic regime the theoretically predicted equidistancy in frequency (solar-type oscillations), or in periods (g modes) serves as a good basis, although with shortcomings (Van Reeth et al. 2014) for algorithmic search (Unno et al. 1981; Aerts et al. 2010). For the low order p modes we do not have such definite guidelines given by the theory.

As a basic idea, we checked the frequency difference between the frequencies of highest amplitude pairs. When the pairs had a similar spacing and one member of the pair appeared in the other pair(s), we regarded them as a starting point of a sequence. Finding frequencies of lower amplitude with a similar spacing, the sequence was extended to higher and lower direction of the frequency range. The frequency pairs that did not connect to the first sequence were used as the starting point for another sequence. We found 1, 2, 3 and 4 sequences for 19, 18, 17 and 10 stars, respectively. For 4 stars, 5 sequences were identified, while for 3 stars, 6 sequences were identified, by visual inspection. The sequences are shifted

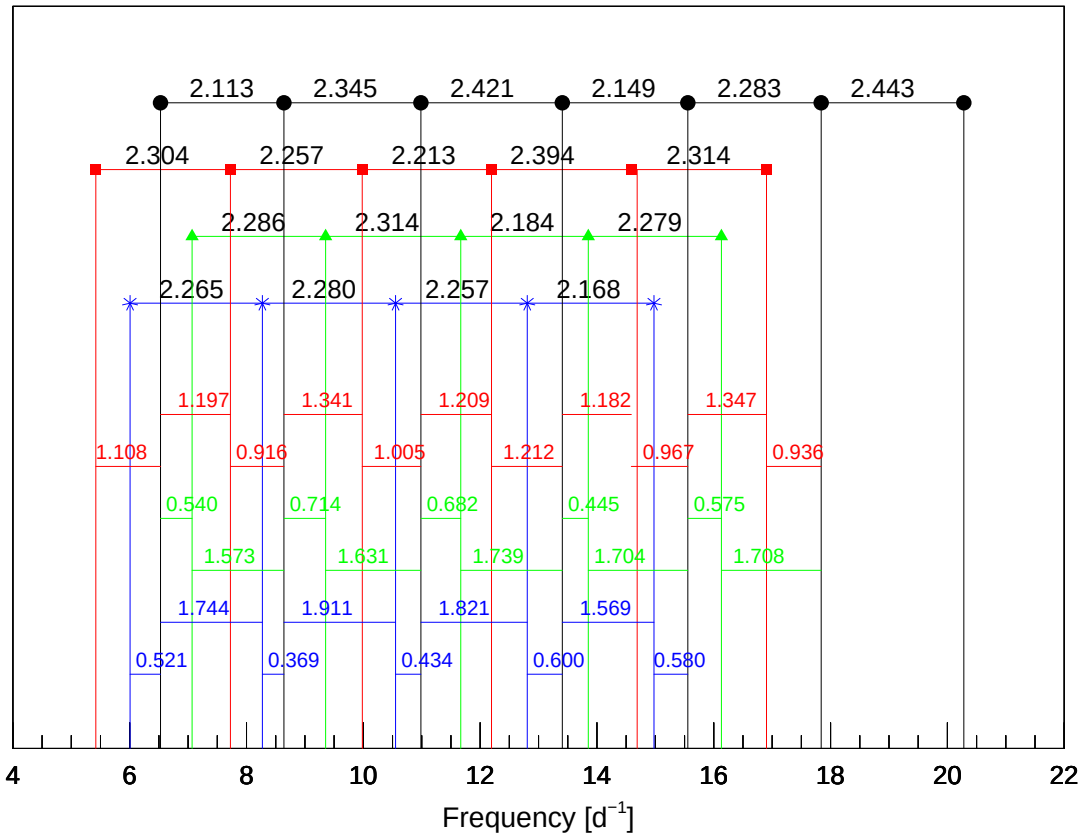

FIG. 1.— Sequences with quasi-equal spacing, and shifts of the sequences for CoRoT 102675756. 1st – black dots, average spacing 2.292±0.138 d^{-1}; 2nd – red squares, 2.296±0.068 d^{-1}; 3rd – green triangles, 2.265±0.057 d^{-1}; 4th – blue stars, 2.242±0.051 d^{-1} average spacing was obtained. The mean spacing of the star is 2.277±0.088 d^{-1}. The shifts of the 2nd, 3rd and 4th sequences relative to the first one are also given in the same color as the sequences.

with respect to each other.

We present here only one case. Fig. 1 shows the four sequences of similar regular spacing for CoRoT 102675756. The sequences consist of 7, 6, 5 and 5 members, respectively, altogether including more than 50% of the filtered frequencies. In this case, each consecutive member of a sequences is excited with amplitude above the accepted limit (in general 0.1 mmag. The amplitude limitation was introduced to avoid the increasing complexity of the frequency distribution at lower amplitude levels.) In other cases, however, we allowed to skip one member of the sequence, if we did not find it, but if half of the second consecutive member's spacing matched the regular spacing. Fig. 1 also displays the independent spacing values between the successive members of the sequence. The mean value of the spacing is independently given for each sequence in the figure caption. The mean values differ only in the second digits. The general spacing value, which is the average of the sequences, is 2.277±0.088 d^{-1}. The deviation of the individual spacings from the mean value in CoRoT 102675756 and in other targets suggests that we may use ±0.1 d^{-1} tolerance in the algorithmic search. With this knowledge we could reduce the standard deviation of the spacing to half of the value given by García Hernández et al. (2009).

The shift of the sequences does not seem to be randomly distributed, but represents characteristic values. For CoRoT 102675756, we present the shifts of the appropriate members of the shifted sequences to the appropriate member (before and after) of the first sequence, used as a reference. The frequencies of the second sequence are almost mid-way between those of the first sequence, what we expect in a comb-like structure of stars pulsating in the asymptotic regime. Exactly, the averaged shift of the second sequence relative to the first is 1.024 d^{-1} to the left. However, the differences do not steadily increase when we move to the higher radial orders. The most plausible explanation at this level would be that we directly see the large separation, and the different echelle ridges have a different order, l, but the situation is probably more complicated, due to the rotation. The members of the two other sequences are asymmetric, one of them is closer to the nth, the other to the $n+1$th member of the first sequence. We derived the shifts for

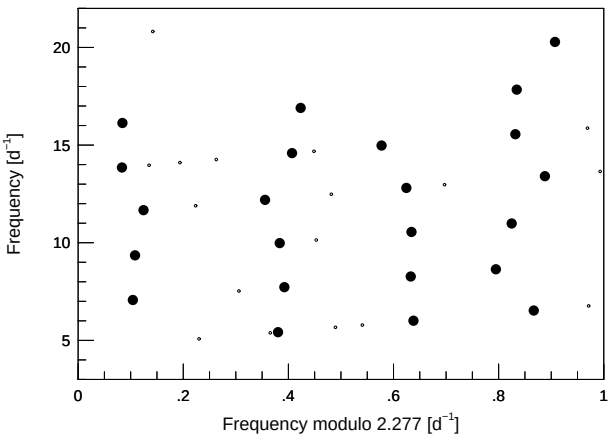

FIG. 2.— Echelle diagram of star CoRoT 102675756, consistent with the sequences of Fig. 1 result of the visual inspection). The mean spacing of the star was used as a modulo frequency. The whole frequency content of the star is plotted (small and large dots). The larger dots show the vertical representation of the sequences, the echelle ridges.

our all targets in this concept for finding any regularity in it and comparing them to the frequency spacings. In our present case, however, even more regularity appears in the shifts. The fourth sequence is also shifted to midway compared to the third sequence. If we calculate the averaged shift of the fourth sequence relative to the third one, we get a 1.092 d^{-1} shift to the left. The third sequence relative to the first one and the second relative to the fourth one are on average shifted to the right by 0.591 and 0.539 d^{-1}, respectively. In addition, the fourth sequence is shifted relative to the first one by 0.501 d^{-1} to the left.

The echelle diagram (a vertical representation of the sequences) is nowadays extensively used in asteroseismology as a valuable way of displaying periodic spacing. The echelle diagram (frequency versus frequency modulo 2.277 d^{-1}) is presented in Fig 2. for CoRoT 102675756, in agreement with the result of the visual inspection. The first, second, third and fourth sequences correspond to the echelle ridges at 0.85, 0.38, 0.1 and 0.65 d^{-1} modulo values. The curvature of the echelle ridges shows the slightly smaller or larger value of the actual spacing between the successive frequencies, but it shows a high level of regularity. It is especially worthwhile to emphasize that the echelle ridges start from the low frequency region of the generally accepted frequency region of δ Scuti stars (Balona & Dziembowski 2011). They cover 4-5-6 large separation regions if we interpret the spacing between the frequencies as the large separation. The ridge with the highest frequency is still well below the asymptotic regime of the p modes. We found four rather straight echelle ridges in the regime where only 1-2 echelle ridges were found by Barban et al. (2001) and García Hernández et al. (2015). Never have been so many frequencies arranged along the echelle ridges in a δ Scuti star as we found for CoRoT 102675756.

The small dots represent frequencies that are not located on any ridges. According to the ray dynamic approach of rapidly rotating stars these modes are not island modes.

According to the AAO spectral classification (Guenther et al. 2012; Sebastian et al. 2012), CoRoT 102675756 has $T_{\rm eff}$=7350±300 K, $\log g$=3.2±0.5 and A7III spectral type and a variable star classification as a γ Dor type star (Debosscher et al. 2009). Following the process used by Balona et al. (2015) for *Kepler* stars, we derived a possible equatorial rotational velocity (100 kms^{-1}). Using the formula of Torres et al. (2010) for the radius, we derived a first order rotational splitting (0.269 d^{-1}).

The three shifts of the four sequences (the second relative to the fourth, the fourth relative to the first and the first relative to the third are 0.539, 0.501 and 0.591 d^{-1}, respectively) could be interpreted as twice the value of the rotational splitting. The appearance of twice the value of the rotational frequency is predicted by theory (Lignières et al. 2010). We wonder whether the shifts of the second sequence relative to the first (1.024 d^{-1}) and the fourth relative to the third (1.092 d^{-1}) represent a higher multiple of the rotational frequency or are instead connected to the odd and even parity in the ray dynamic approach.

The echelle ridges start at 5 d^{-1}, near the γ Dor frequency range. However, these regularities appear in frequencies, and not in periods as we would expect for g modes of γ Dor stars. The star could be a p-mode/g-mode hybrid like those discovered by space missions (Uytterhoeven et al. 2011); however, Hareter (2013) classified it as a pure δ Scuti stars with no hybrid character.

The regular structure of the shifted sequences is so obvious (at least for one of us) that already the visual inspection recognized sequence(s) in most of our targets.

2.2. *Algorithmic search (SSA)*

Of course, the visual inspection of a larger sample is very time-consuming. However, detecting non-uniform period spacing can be rather complicated, especially if two different series with a different average spacing overlap, as Van Reeth et al. (2014) discuss for γ Doradus stars. Based on the constraints of the visual inspection (possible range of spacing, value of tolerance) we developed an algorithm (SSA) to automate the process. The main steps of the algorithm are illustrated by the schematic flow chart in Fig. 3.

The SSA uses the same frequency lists as input data as we use for VI. (1) First, if incidentally some too-close frequency pairs remained (viz. within the range of tolerance $\Delta f = \pm 0.1$ d^{-1}) in the filtered frequency lists, we remove the lower amplitude compliments. This means few (1-5) frequencies for a couple of stars. (2) We calculate the mutual distances between each pair for the ten highest amplitude frequencies. Then we omit those distances which are out of the possible spacing range determined by VI (1.35-8 d^{-1}). (3) The algorithm constructs a spacing grid consisting of the proper distances and fine grids around each such distance. The fine grid allows us to find those sequences in which the average spacing is slightly different from any of the exact distances between the frequency pairs within the sequence. (4) The core process of the algorithm searches for sequences at each grid point. (i) The search starts with the highest amplitude frequency (basis frequency) and tries to find

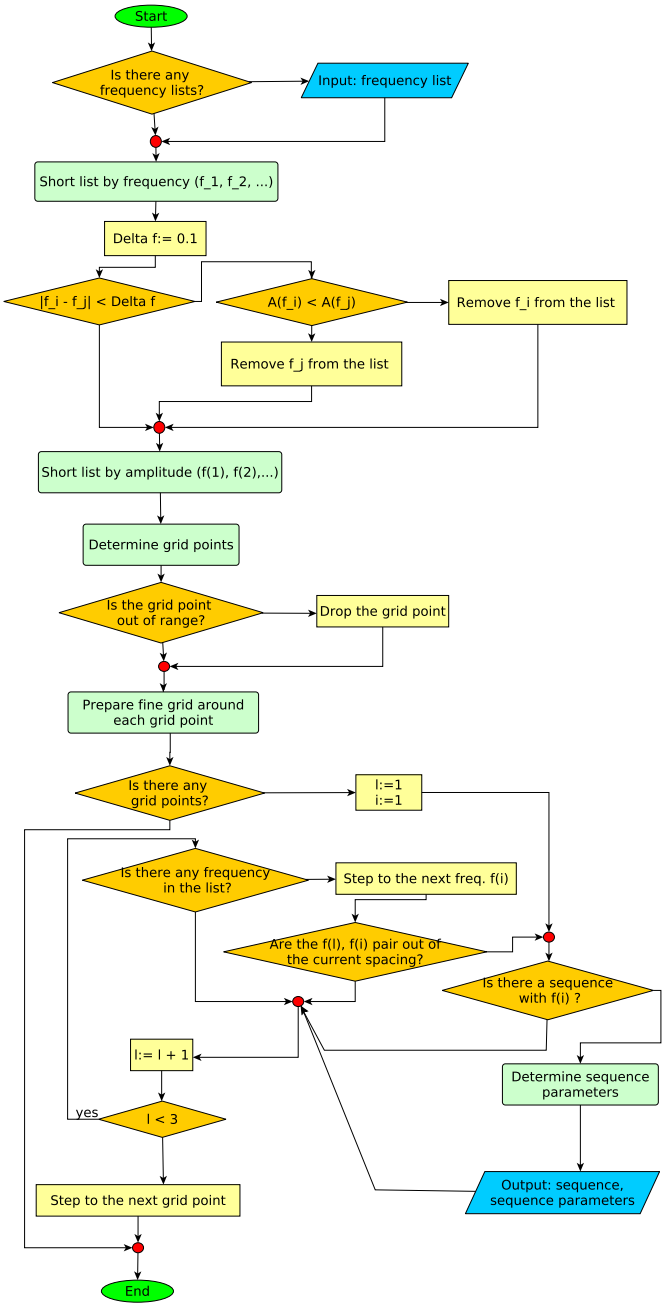
Start
Is there any frequency lists?
Input: frequency list
Short list by frequency (f_1, f_2, ...)
Delta f:= 0.1
|f_i - f_j| < Delta f
A(f_i) < A(f_j)
Remove f_i from the list
Remove f_j from the list
Short list by amplitude (f(1), f(2),...)
Determine grid points
Is the grid point out of range?
Drop the grid point
Prepare fine grid around each grid point
Is there any grid points?
l:=1
i:=1
Is there any frequency in the list?
Step to the next freq. f(i)
Are the f(l), f(i) pair out of the current spacing?
Is there a sequence with f(i) ?
l:= l + 1
Determine sequence parameters
yes
l < 3
Step to the next grid point
Output: sequence, sequence parameters
End

FIG. 3.— Schematic flow diagram of our Sequence Search Algorithm (SSA). The convention in this plot is that the rightwards pointing arrows of the conditional boxes show the 'yes' destinations and the downward pointing ones show the 'no' conditions. See the text for the details.

an at least four element frequency sequence, where the elements of the sequence are located at the actual spacing within the value of tolerance. If the SSA find a sequence it calculates some parameters such as the deviation of the sequence from the exact equidistant spacing, and the sum of the amplitude of the component frequencies. (ii) The search continues with the closest neighbor frequency to the previously used ones, except it is farther on the basis frequency than the actual spacing. In the first case we can find additional (shifted) sequences for the given spacing. In the latter case we change the basis frequency to the second highest amplitude frequency and re-start the search. According to the results of the VI we do not use the lower amplitude frequency as the basis one. (5) At the end, we compare the parameters of the found sequences and determine the dominant spacing, where we found the most number of sequences and/or the most frequencies in sequences. If we have similar results for some different spacings we take into account additional parameters (amplitude sums, standard deviation) for choosing the dominant spacing.

Using all frequencies in the algorithmic search, we found slightly more sequences (even 7 or 8), although the requirements were more severe than in the visual inspection, but the search is more systematic. For CoRoT 102675756 the SSA determined five sequences compared to the four sequences obtained by VI, showing that SSA does not exactly reproduce the results of the visual inspection. In many cases SSA found more than one almost equally valid dominant spacing. For CoRoT 102675756 both 2.249 and 1.977 d^{-1} spacings were found. The difference of the two spacings (0.272 d^{-1}) numerically agrees with the rotation frequency (0.269 d^{-1}). Calculating the modulo value for the 2.249 d^{-1} spacing, the echelle ridges appear at 0.14, 0.42, 0.55, 0.69 and 0.90 values, while the echelle ridges calculated with 1.977 d^{-1} are at 0.03, 0.13, 0.37, 0.55 and 0.90. This means that four of them appear at the same modulo value, and only one ridge is different. 17 frequencies appear in ridges for both spacing but they are located on different ridges. In the echelle diagram we do not see the rotationally split frequencies as parallel ridges as is the case for the asymptotic regime for a sequence of consecutive radial orders. This suggests that none of the ridges represent frequencies with the same l value and cannot be trivially interpreted as the large separation.

2.3. *Fourier Transform (FT)*

At the introduction of a new method it is always desirable to compare it to a previously used method. We prepared the FT of our targets and derived the spacing as the highest peak. We followed the way described by Handler et al. (1997). The frequency content with unit amplitudes is the input data for getting the spectral window of the frequency distribution. The time domain is transferred again to the frequency domain and the amplitudes to power. We applied the definition of the Nyquist frequency omitting the low-frequency region of FT.

The highest peak of the FT of CoRoT 102675756, 2.137 d^{-1}, is pretty much equal to the spacing of the visual inspection, i.e. 2.277 d^{-1}, or the spacing obtained by the algorithmic search: 2.249 d^{-1}. However, the two methods (three approaches) do not always give as precise agreement as in the presented case. Mostly the visual inspection and the algorithmic search resulted in similar spacings. However, there is full agreement of the spacing obtained by the different approaches only for 13 targets. It is worthwhile to mention the 8 targets where the FT spacing proved to be half of the visual inspection's spacing. These stars show the closest similarity to the spacing in the asymptotic regime.

Fig. 4 summarizes the spacings obtained by the different approaches. The individual spacings derived for 77 δ Scuti stars were binned in 0.5 d^{-1} wide interval. To avoid the overlapping of the histograms, the number in the bin

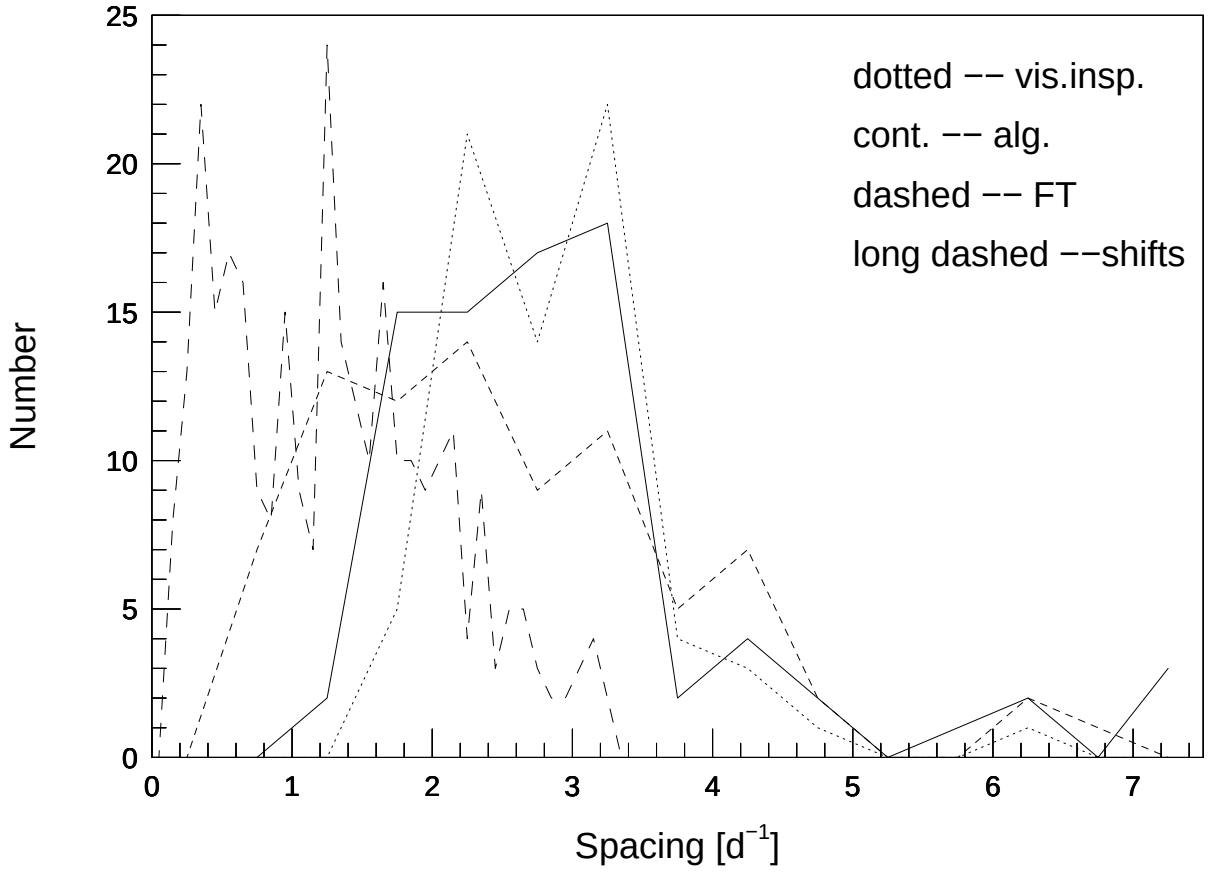

FIG. 4.— Distributions of the spacing derived by visual inspection (dotted line), algorithmic search (continuous line), and Fourier Transform (dashed line) are compared. The latter one has higher numbers at low spacing values. The distribution of the shifts are overplotted by the large dashed line. One of the highest peaks coincides with the large numbers of spacings obtained by FT.

is plotted at the middle of the bin and the points are connected. The total number under a certain type curve gives the number of stars in our sample. The distribution of the spacings is only slightly different for the visual inspection (dotted line) and algorithmic search (continuous line) (1.5-3.8 d^{-1}) but FT (dashed line) shows a remarkably wider distribution (1.0-4.5 d^{-1}), especially in the lower spacing values. In these distributions we applied the spacing value resulting in echelle ridges with less scatter, although in many targets more than one spacing appeared, mostly around the two pronounced peaks of the visual inspection's spacing.

We conclude that the different approaches (with different requirements) are able to catch different regularities among the frequencies. The different spacing values are not the mistake of any of the methods; rather the methods are sensitive to different regularities. The visual inspection and the algorithmic search concentrate on the continuous sequences, while the FT is more sensitive to the number of similar frequency differences. When we have a second sequence with a mid-shift, then the FT shows that, instead of the spacing of a single sequence, the spacing will be twice the value of the highest peak in the FT.

If the shifts of the sequences are asymmetric, the FT shows a low and a larger value with equal probability. When we have many peaks in the FT then we have many echelle ridges with different shifts with respect to each other. The sequence method helps to explain the fine structure of the Fourier Transform.

The shifts derived between the sequences (if there is more than one) are a fraction of the spacings. It could be worthwhile to compare their distribution to that of the spacing.

We overplotted the distribution of the shifts in Fig. 4 by the long dashed line. The shifts are more numerous that the spacing. Their number depends on the number of the echelle ridges. Although we averaged them in a sequence, six shifts appears in the case of four echelle ridges as Fig. 1 shows. The shifts are binned in 0.1 d^{-1} intervals. Only the numbers in a bin versus the center frequencies of the bin are plotted, as in the case of the spacings. The plot shows two dominant peaks at 0.35 and 1.25 d^{-1}. The latter coincides with a peak of FT spacing showing that in many cases the FT shows the shift of the sequence instead of the spacing of a single

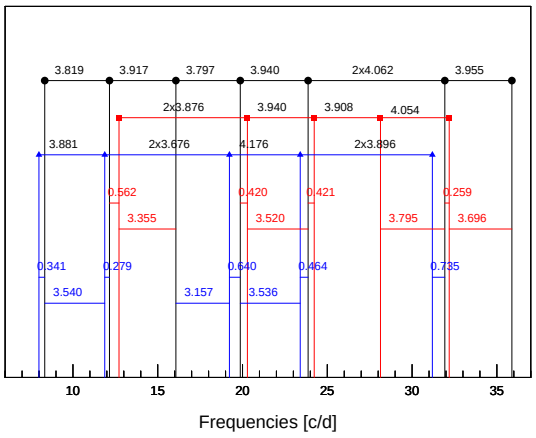

FIG. 5.— Sequences among the observed frequencies of FG Vir that is one of the best-studied δ Scuti star. The sequences are presented in black, red and blue colors. Some members are missing and the small shifts of the sequences with respect to each other strengthen the feeling of grouping of frequencies. The shifts of the members of a sequence with respect to the first one are plotted with the same color as the sequence.

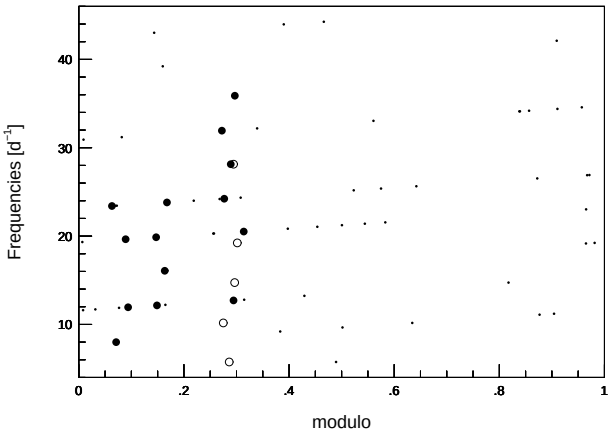

FIG. 6.— Echelle diagram of the observed frequencies of FG Vir calculated by 3.86 d^{-1} (full large dots). The background points are all the independent frequencies. Only 21% of the frequencies are located on the echelle ridges. Open circles delineate the echelle ridge calculated by the 4.47 d^{-1} spacing. A side peak of FG Vir in the FT is shown in the next figure.

sequence.

3. DISCUSSION

The basic question is why we have so many sequences in our targets. What is the origin of the different regularities obtained in a star? We have found many reasons for producing regularities in the frequencies of pulsating stars.

The alias structure as a possible source of the regularity was ruled out after detailed examination of the spectral window of the light curves. The other possible source, the linear combination, was also excluded, since only a few linear combination appeared and they did not belong to the echelle ridges. Only one target's single echelle ridge was excluded due to linear combination.

In a pulsating star, however, the consecutive radial orders with an l value represent a sequence of frequencies with a regular spacing (although not exactly equidistant). The radial orders of different l value frequencies can represent different sequences with the same spacing. The simplest explanation would be that the different echelle ridges represent sequences with different l value. However, in some cases we have seven or even eight echelle ridges. Due to the geometrical cancellation, it is not very probable that we can observe modes with so high l value. We therefore conclude that regular spacing can appear due to consecutive radial orders but it is definitely not the only origin.

We tried to apply the theoretical period ratio of the radial fundamental and first overtone for the identification of a sequence with l=0. The appearance of the radial period ratio depends on the spacing value, the most popular being the 2.1-2.9 d^{-1} spacing regions with (7.1-10.24)/(9.1-13.12) frequency region for possible radial fundamental and first overtone period ratio. However, these pairs did not agree with the first two members of the echelle ridges, so we could not use them to localize radial modes.

According to the perturbative theory, the rotational

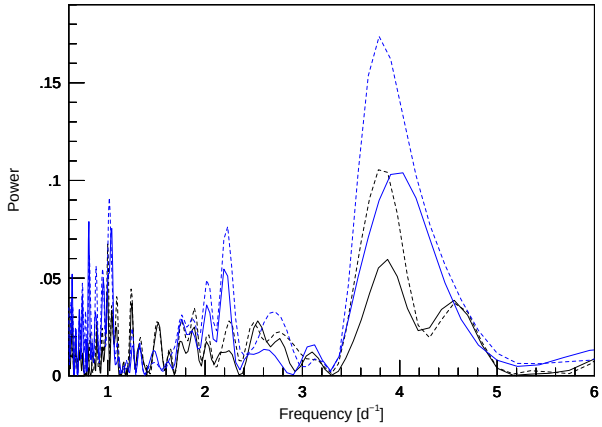

FIG. 7.— FT of the observed modes in FG Vir. We prepared five different subsets using a color code for compact presentation. Black continuous line – all observed frequencies, black dashed line – independent frequencies, blue continuous line – all frequencies above 0.4 mmag, blue dashed line – independent frequencies above 0.4 mmag.

splitting modifies the regular sequence of eigenmodes. At slow rotation the splitting value is lower and has an equidistant structure. For fast rotators the splitting structure is more complex, quintuplets are overlapped and they are not equidistant due to the second-order effects. The ray dynamic approach revealed different classes of modes with different characteristics concerning regularities. Fig. 6. of Ouazzani et al. (2015) presented altogether nine echelle ridges (three for the non-rotating case and six for the rotating case) for $\hat{l}$ = 0, 1 and 2 island modes (which are the counterparts of the low order acoustic modes) with odd and even parity. With the odd and even parity the number of the echelle ridges is doubled. Some of the echelle ridges are overcrossed. Due to

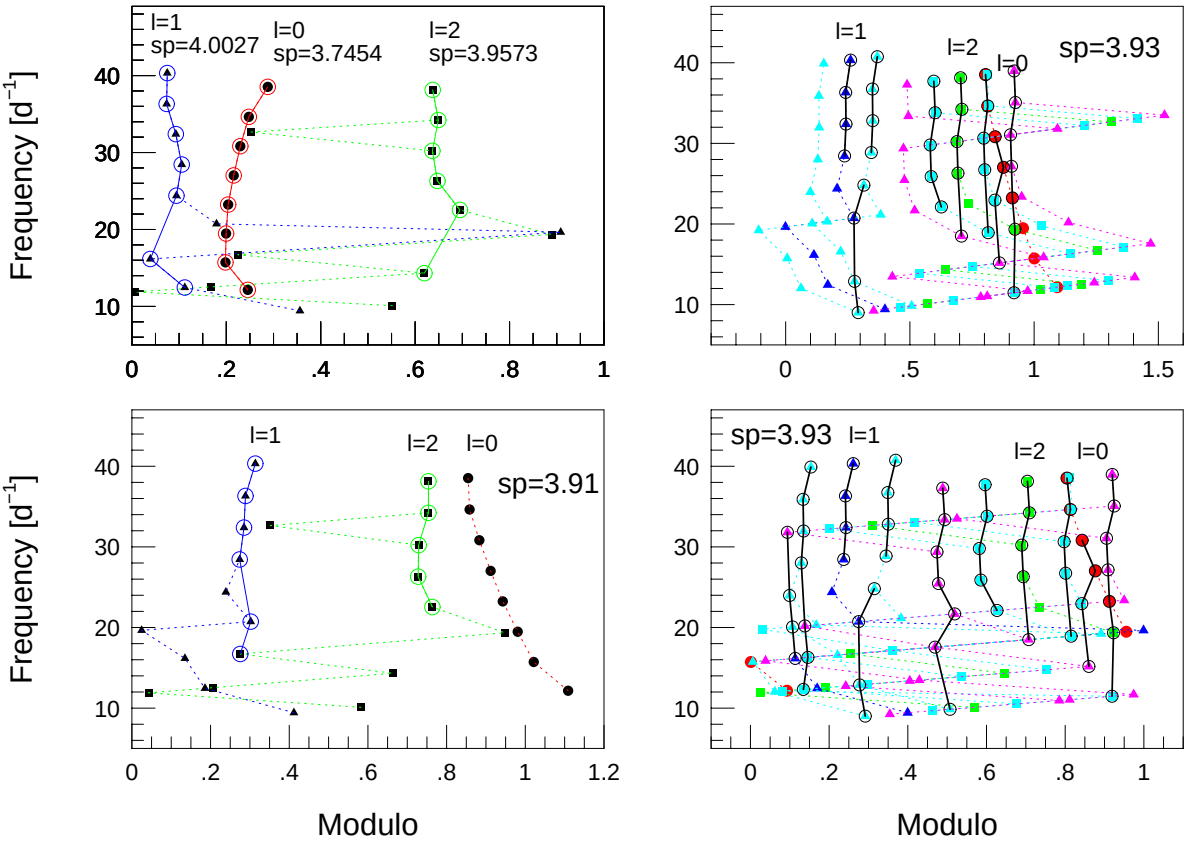

FIG. 8.— Echelle diagrams of model frequencies of FG Vir. Spacings were obtained independently for l=0, 1 and 2 modes (left, top panel) and altogether (left, bottom panel). The actual spacings are labeled in the panels. Right panels show the rotationally split frequencies in two representations: modulo values are shifted by $\pm$ 1 d^{-1}, if it is necessary (top panel) and what we see in a real star (bottom panel). Color code: red, blue and green colors are used for l=0, 1 and 2 modes, respectively. The rotationally split triplets are represented by light blue, while the multiplet members by magenta.

the curvature in the low and high frequency region and the overcrossing region, our tolerance limit could not recognize and resolve all echelle ridges in their model.

Of course, a final solution could be a pulsational modeling of a real star with their ACOR code (Ouazzani et al. 2012). It seems that we are close to this level of interpreting intermediate and fast rotating stars. However, first, we checked our sequence search method for the first order rotationally split modes of the best observed δ Scuti star, FG Vir.

3.1. *FG Vir as a check star*

A trivial check is the application of our sequence search method for the observed frequencies of a well-studied δ Scuti star and for $l = 0, 1, 2$ eigenmodes of its modeling. FG Vir is one of the best studied δ Scuti stars from both the observational (photometry and spectroscopy) and from the theoretical side. Our sequence search method (both the visual inspection and algorithmic search) was applied for 75 observed frequencies were taken from Breger et al. (2005). The sequences, using the independent frequencies, were prepared by visual inspection. Fig. 5 shows 17 frequencies in three sequences with 3.931$\pm$0.122 d^{-1} mean spacing. The second and the third sequences are slightly shifted with respect to the first one. Some of possible members of the sequences are not excited over the amplitude limit. It is quite understandable that FG Vir was one example of a δ Scuti star showing groups of frequencies. The shifts of the second and third sequences relative to the first one on average are 0.414 and 0.491 d^{-1}, respectively. Concerning the 0.423 d^{-1} rotational frequency of FG Vir obtained by Mantegazza et al. (1994), this shift should be interpreted as the rotational splitting of triplets. The triplets introduce a spacing that is the sum of the large separation and the rotational splitting. Regarding the prograde or retrograde component of a triplet, or the components of a multiplet structure, another possible spacing is the sum of the large separation and twice the value of the rotational splitting.

The algorithmic search revealed 3.86 d^{-1} spacing for the observed frequencies in good agreement with the 3.7

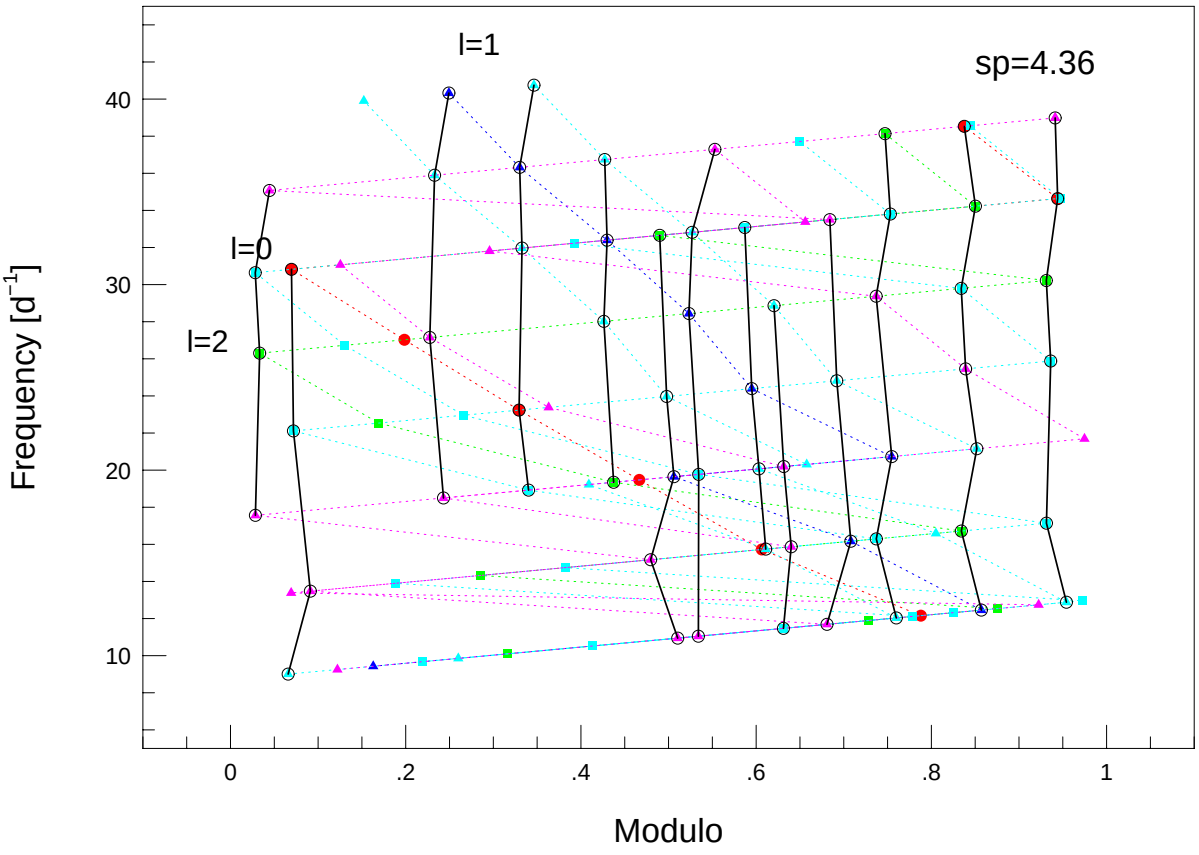

FIG. 9.— Echelle diagrams of model frequencies of FG Vir modulo 4.36 d^{-1}. The search for regular spacing resulted also in a second spacing, that we used here. The color code shows that the echelle ridges contain frequencies with different degrees l and also the rotationally split frequencies too. The second spacing is the sum of the first spacing (3.93 d^{-1}) and the $f_{\rm rot} = 0.4234$ d^{-1}. The color code is the same as in Fig. 4.

d^{-1} spacing published by Breger et al. (2009). Fig. 6 shows the echelle diagram with 3.86 d^{-1} spacing obtained by SSA. The sporadic distribution (not more than three members of a possible echelle ridge) does not fulfill our requirements for SSA. Three echelle ridges with 14 frequencies (full dots) are shown. Open circles show an overplotted echelle ridge that was calculated using a 4.47 d^{-1} spacing, which is the second spacing obtained by SSA. This spacing represents the sum of the large separation and the rotational frequency, although it has a slightly larger value than the 0.432 d^{-1} rotational frequency obtained by Mantegazza et al. (1994).

We also applied the FT for the observed frequencies. We checked two effects, the linear combination frequencies and the effect of the lower amplitude frequencies, for the FT. Fig. 7 gives a compact representation of our results. We prepared the FT for the following data sets: all the observed frequencies of FG Vir (black continuous line), only the independent frequencies (black dashed line), all frequencies above 0.4 mmag amplitude (48 frequencies, blue continuous line) and the independent frequencies above 0.4 mmag amplitude (42 frequencies, blue dashed line). The dominant features of the curves are the dominant peaks at around 3.9 d^{-1} in all subsets. Concerning the dominant peaks we can conclude that the black lines (both continuous and dashed) reflect a second lower peak at 4.56 d^{-1}, in addition to the dominant spacing. Comparing this value to the second spacing of FG Vir obtained by SSA (4.47 d^{-1}), we may interpret this second spacing as the sum of the large separation and the rotational frequency. Using only the high amplitude modes (blue lines) we miss the side peak of the FTs, but the dominant peaks have a larger width covering the second peaks of the FT. It seems to be plausible that the rotationally split modes have a lower amplitude. The other effect is that the subsets using only the independent modes have a dominant peak with a higher amplitude.

The FG Vir model that we used here (see Guzik et al. 2000 for modeling details) was evolved using the OPAL opacities with Grevesse & Noels (1993) abundance mixture, initial helium mass fraction Y=0.28, and mass fraction of elements heavier than hydrogen and helium, Z, of 0.02. It has $T_{\rm eff}$ = 7419 K, L = 13.92 L$_\odot$, and

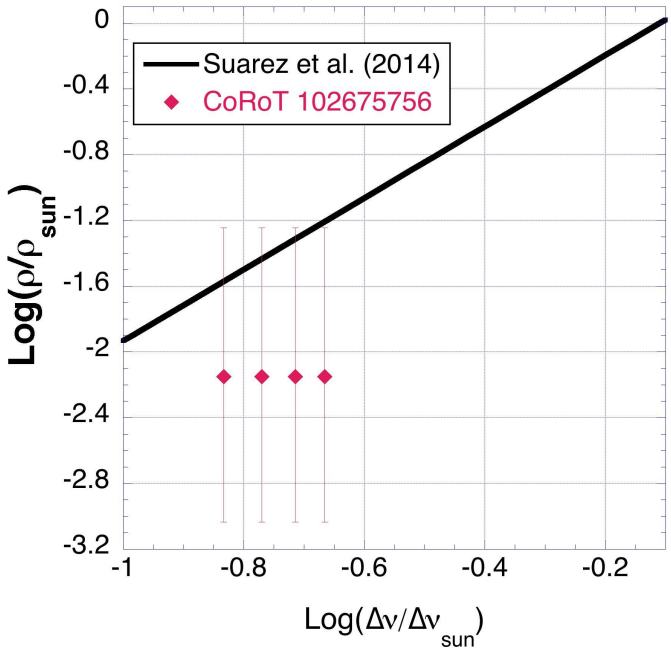

FIG. 10.— The location of the four possible large separation of CoRoT 102675756 on the space density versus large separation diagram given by Suárez et al. (2014). The error bars are calculated based on the error bars of $T_{\rm eff}$ and $\log g$. The $\Delta\nu$=1.710 d^{-1} is the closest point to the straight line.

R=2.26 R$_\odot$.

This model has a main-sequence age of 0.867 Gyr, and a convective core with core hydrogen mass fraction 0.270. Outside the convective core there is a composition gradient where a high Brunt-Väisälä frequency has developed that forms a cavity in which the mode frequency is less than both the Brunt-Väisälä frequency and the Lamb frequency, and where gravity modes can propagate.

For the l = 1 modes, the ten calculated frequencies range from pure p modes with 8 radial nodes at highest frequency, to pure g modes (2 g-type nodes) at lowest frequency. For l = 2, the twelve calculated frequencies range from pure p modes with 7 radial nodes to pure g modes (4 g-type nodes). At intermediate frequencies, the modes may have a mixture of p and g-type nodes. When the g-mode character of the modes begins to dominate, nearly equidistant frequency spacing is altered. For l = 1, this occurs for the lowest frequency modes. For l = 2, this occurs both for the lowest frequencies when the g-mode character dominates, and for the third highest frequency when a g-type node first appears. For l = 0, since these are radial modes, the modes cannot have a nonradial g-mode character, and the calculated frequency spacing follows a regular pattern.

The l=0 , l=1 and l=2 eigenmodes were independently treated, resulting 3.7454, 4.0027 and 3.9573 d^{-1} spacing, respectively. The corresponding echelle ridges are shown in the left, top panel of Fig. 8. The l=0 eigenmodes have a slightly smaller spacing than the l=1 and 2 modes. Applying the method for all eigenmodes, we found a 3.91 d^{-1} spacing and only two echelle ridges (l=1 and 2), presented in the left, bottom panel of Fig. 8. Due to the smaller spacing value of l=0 frequencies, the curvature of the l = 0 frequencies according to modulo 3.91 d^{-1}, did not fulfill the tolerance requirement of SSA.

The test shows that the consecutive radial orders of an l value can represent echelle ridges in our sequence method. However, not all of the eigenmodes (connected by dotted lines) are situated on the echelle ridges and, due to the slightly different spacing of the eigenmodes, we do not find all l ridges at the same time.

The first order rotational splitting of l = 1 modes to triplet and l = 2 modes to a quintuplet structure was derived using a reliable $f_{\rm rot}$=0.4234 d^{-1}, obtained from observation.

Application of the method for the 94 rotationally split modes leads to a more conclusive result for the unexpectedly large number of echelle ridges in our sample. We found two dominant spacings, at 3.93 d^{-1} which is similar in the observed frequencies. The other spacing is 4.36 d^{-1} which is the sum of the previous one and the $f_{\rm rot}$. Since we know how the rotationally split modes were generated, we show two representations for the 3.93 d^{-1} spacing on the right side of Fig. 8. To follow the l=0, 1 and 2 eigenmodes and the rotational splitting clearly, the modulo values were shifted by ±1 as necessary (top panel). The bottom right panel gives the situation that we can see in a real star. The echelle diagram modulo 4.36 d^{-1} spacing is given in Fig. 9. It is obvious that in all cases we see many echelle ridges (8, 11 and 13). The color code shows that the echelle ridge contains not only the consecutive radial orders of an l value, but the rotationally split modes, too. The severe constraint of the tolerance shows that the complex echelle ridges have quasi-equal spacing despite their origin.

We conclude that one spacing reflects the large separation, while the other spacing represents the sum of the large separation and the rotation. We found a good argument for the numerous echelle ridges in δ Scuti stars, even using first order rotational splitting. The echelle ridges do not overcross but we have closely spaced echelle ridges. However, in this case we can resolve them with our ±0.1 d^{-1} tolerance level.

What may we conclude for CoRoT 102675756 given the results on the model frequencies of FG Vir? Although the difference of the two spacings for CoRoT 102675756 (2.249 and 1.977 d^{-1}) agrees with the estimated rotational splitting (0.269 d^{-1}) we may not be sure that one of the spacings reflects the large separation, itself, or instead a combination of the large separation and the rotational frequency. Taking into account that the appearance of the rotational frequency and/or double its value have been found in the auto-correlation of the frequency spectrum (Lignières et al. 2010), we have the following possibilities as an explanation:

$$SP_1 = \Delta\nu, \text{ and } SP_2 = \Delta\nu - \Omega_{\rm rot},$$
$$SP_2 = \Delta\nu, \text{ and } SP_1 = \Delta\nu + \Omega_{\rm rot},$$
$$SP_1 = \Delta\nu + 2\cdot\Omega_{\rm rot}, \text{ and } SP_2 = \Delta\nu + \Omega_{\rm rot},$$
$$SP_2 = \Delta\nu - 2\cdot\Omega_{\rm rot}, \text{ and } SP_1 = \Delta\nu - \Omega_{\rm rot},$$

where, SP_1 and SP_2 are the larger and smaller values of the spacings, respectively, found by SSA, $\Delta\nu$ is the large separation in the traditionally used sense, namely, the differences between the consecutive radial orders with the same spherical degree, and $\Omega_{\rm rot}$ is the estimated rotational frequency.

In all cases $SP_1 - SP_2 = \Omega_{\rm rot}$, the estimated rotational

frequency of CoRoT 102675756. Using $SP_1 = 2.249$ d^{-1}, $SP_1 = 1.977$ d^{-1} and $\Omega_{\rm rot} = 0.269$ d^{-1}, we get four possible value for the large separation ($\Delta\nu$) of CoRoT 101675756, namely 2.249, 1.977, 1.710 or 2.517 d^{-1}.

Fig. 8 shows how these possible large separations are related to the relation between the mean density and the large separation given by Suárez et al. (2014). We obtained the mean density of CoRoT 102675756 using the formulas of Torres et al. (2010) for mass and radius, given $T_{\rm eff}$ and $\log g$ and their uncertainties, and assuming solar metallicity. Since we do not have special single-star oriented spectroscopy, the error bars are rather large. Nevertheless, the $\Delta\nu$=1.710 d^{-1} is located at the closest place to the relation. This means that the larger spacing value gives the sum of the large separation and twice the value of the rotational frequency, while the smaller spacing represent the sum of the large separation and the rotational frequency.

4. CONCLUSION

None of the three approaches, visual inspection, algorithmic search or Fourier Transform, can give a unique spacing for many stars. In the simplest cases (one or two ridges) the spacing values are the same for all methods. When we have a complex spacing structure, then it may happen that any two of the three methods agrees, but sometimes all of them produce a different spacing. This seemingly contradictory result means that the methods (with different requirements) are more sensitive to one of the characteristic spacings.

The benefit of the sequence search method is that, beside obtaining the spacing value(s), we immediately know how many sequences are found in the star. The shifts between sequences provide more insight into the pulsation-rotation interaction, especially when the shifts agree with the rotational frequency or twice its value. High quality spectra providing accurate physical parameters ($\log g$, $T_{\rm eff}$, metallicity, and rotation rate) would be enough to interpret the spacings and obtain the seismic parameters of any large sample of δ Scuti stars.

The application of the sequence search method for the model frequencies of FG Vir was especially informative. For the rotationally split set of frequencies, the sequence search method revealed many echelle ridges showing that frequencies of different origin (consecutive radial orders or rotationally split frequencies) are located on the same echelle ridges with the same spacing. The two spacings found, 3.93 and 4.36 d^{-1}, proved to be the large separation and the sum of the large separation and the rotational frequency. For our sample target, CoRoT 102675756, both spacings (2.249 and 1.977 d^{-1}) seem to be the combination of the large separation and the rotational frequency. The explanation that $2.249 = \Delta\nu + 2 \cdot \Omega_{\rm rot}$ and $1.977 = \Delta\nu + \Omega_{\rm rot}$ seems to be more plausible, resulting in a 1.710 d^{-1} large separation, because it fits better the Suárez et al. (2014) relation.

Our whole sample will be published in more detail in Paparó et al. (2015). We have good hope to make progress in the resolution of rotation and pulsation, reaching the asteroseismology level, too, in the non-asymptotic regime.

This work was supported by the grant: ESA PECS No 4000103541/11/NL/KLM.

REFERENCES

Aerts, C., Christensen-Dalsgaard, J., & Kurtz, D. W. 2010, Asteroseismology, A&A Library, (Berlin - Heidelberg: Springer)

Auvergne, M., Bodin, P., Boisnard, L., et al. 2009, A&A, 506, 411

Baglin, A., Auvergne, M., Barge, P., et al. 2006, in ESA SP 1306, The CoRoT Mission Pre-Launch Status - Stellar Seismology and Planet Finding, ed. M. Fridlund, A. Baglin, J. Lockhard, & L. Conroy, (Noordwijk: ESA), 33

Balona, L. A., & Dziembowski, W. A. 2011, MNRAS, 417, 591

Balona, L. A., Daszynska-Daszkiewicz, J. & Pamyatnykh, A.A. 2015, MNRAS, 437, 1476

Barban, C., Goupil, M.-J., Van't Veer-Menneret, C., & Garrido, R. 2001, in ESA SP 464, Proc. SOHO 10/GONG 2000 Workshop, ed. A. Wilson, (Noordwijk: ESA), 399

Borucki, W. J., Koch, D., Basri, G., et al. 2010, Science, 327, 977

Breger, M., Pamyatnykh, A. A., Pikall, H., & Garrido, R. 1999, A&A, 341, 151

Breger, M., Lenz, P., Antoci, V., et al. 2005, A&A, 435, 955

Breger, M., Lenz, P., & Pamyatnykh, A. A. 2009, MNRAS, 396, 291

Breger, M., Balona, L., Lenz, P., et al. 2011, MNRAS, 414, 1721

Chen, X. H., & Li, Y. 2015, arXiv:1508.03916

Deupree, R. G. 2011, ApJ, 742, 9

Debosscher, J., Sarro, L. M., López, M., et al. 2009, A&A, 506, 519

Dziembowski, W. A., Balona, L. A., Goupil, M.-J., & Pamyatnykh, A. A. 1998, in The First MONS Workshop: Science with a Small Space Telescope, ed. H. Kjeldsen, & T. R. Bedding, (Århus: Århus Univ.), 127

Fox Machado, L., Pérez Hernández, F., Suárez, J.C., et al. 2009, A&A, 446, 611

García Hernández, A., Moya, A., Michel, E. et al. 2009, A&A, 506, 79

García Hernández, A., Moya, A., Michel, E. et al. 2013, A&A, 559, A63

García Hernández, A., Lignières, F., Balona, L., et al. 2015, in EPJ Web of Conf. 101, The Space Photometry Revolution, ed. R. A. García, & J. Ballot, id.06026

Garrido, R. 2000, in ASP Conf. Ser. 210, Delta Scuti and Related Stars, ed. M. Breger & M. H. Montgomery, (San Francisco, CA: ASP), 67

Goupil, M.-J., Dupret, M. A., Samadi, R., et al. 2005, J. Astrophys. Astron., 26, 249

Grevesse, N., & Noels, A. 1993, Physica Scripta, T47, 133

Guenther, E. W., Gandolfi, D., Sebastian, D., et al. 2012, A&A, 543, A125

Guzik, J. A., Bradley, P. A., & Templeton, M. R.. 2000, in ASP Conf. Ser. 210, Delta Scuti and Related Stars, ed. M. Breger & M. H. Montgomery, (San Francisco, CA: ASP), 247

Handler, G., Pikall, H., O'Donoughue, D., et al. 1997, MNRAS, 286, 303

Hareter, M. 2013, PhD Thesis, Univ. Vienna, Austria

Jackson, S., McGregor, K.B., & Skumanich, A. 2004, ApJ, 606, 1196

Kurtz, D. W., Saio, H., Takata, M., et al. 2014, MNRAS, 444, 102

Lignières, F., Rieutord, M., & Reese, D. R. 2006, A&A, 455, 607

Lignières, F., & Georgeot, B. 2008, Phys. Rev. E, 78, 6215

Lignières, F., & Georgeot, B. 2009, A&A, 500, 1173

Lignières, F., Georgeot, B., & Ballot, J. 2010, Astron. Nachr., 331, 1053

Mantegazza, L., Poretti, E., & Bossi, M. 1994, A&A, 287, 95

Mantegazza, L., Poretti, E., Michel, E., et al. 2012, A&A, 542, A24

Matthews, J. M. 2007, CoAst, 150, 330

McGregor, K. B., Jackson, S., Skumanich, A., & Metcalf, T. S. 2007, ApJ, 663, 560

Ouazzani, R.-M., Dupret, M.-A., & Reese, D. R. 2012, A&A, 547, A75

Ouazzani, R.-M., Roxburgh, I. W., & Dupret, M.-A. 2015, A&A, 579, A116
Paparó, M., Bognár, Zs., Benkő, J. M., et al. 2013, A&A, 557, A27
Paparó, M., Benkő, J. M., Hareter, M., & Guzik, J. A. 2015, ApJS (submitted)
Reese, D. R., Lignières, F., & Rieutord, M. 2006, A&A, 455, 621
Reese, D. R., Lignières, F., & Rieutord, M. 2008, A&A, 481, 449
Reese, D. R., Thompson, M. J., MacGregor, K. B., et al. 2009, A&A, 506, 183
Roxburgh, I. W. 2006, A&A, 454, 883
Saio, H., Kurtz, D. W., Takata, M., et al. 2015, MNRAS, 447, 3264
Sebastian, D., Guenther, E. W., Schaffenroth, V., et al. 2012, A&A, 541, A34
Suárez, J. C., Goupil, M.-J., Reese, D. R., et al. 2010, ApJ, 721, 537
Suárez, J. C., García Hernández, A., Moya, A., et al. 2014, A&A, 563, A7
Torres, G., Andersen, J. & Gimenéz, A. 2010, A&A Rev., 18, 67
Unno, W., Osaki, Y., Ando, H, et al. 1981, Nonradial Oscillations of Stars, (Tokyo: Univ. of Tokyo Press), 2nd ed.
Uytterhoeven, K., Moya, A. Grigahcène, A., et al. 2011, A&A, 534, A125
Van Reeth, T., Tkachenko, A., Aerts, C., et al. 2014, A&A, 574, A17
Viskum, M., Kjeldsen, H., Bedding, T., et al. 1998, A&A, 335, 549
Zahn, J.-P. 1992, A&A, 265, 115